

Time-Dependent Seismic Tomography at the Coso Geothermal Area

Najwa Mhanna¹, Bruce R. Julian¹, Gillian R. Foulger¹, Andrew E. Sabin² and David Meade²

¹Dept. of Earth Sciences, Durham University, Durham DH1 3LE, United Kingdom

²U.S. Navy Geothermal Program Office, China Lake, CA 93555

najwa.mhana@durham.ac.uk; b.r.julian@durham.ac.uk; g.r.foulger@durham.ac.uk; andrew.sabin@navy.mil;
david.meade@navy.mil

Keywords: Seismic tomography; temporal change; Coso;

ABSTRACT

Variation of seismic wave speeds with time is an expected consequence of geothermal exploitation, but detecting and mapping such variation is not straightforward. Three-dimensional structure models derived using seismic tomography are subject to ambiguities caused by incomplete data coverage and observational errors, which can easily exceed any real changes in the wave speeds. Simple comparison of tomographic models based on independent inversions of data from different epochs may thus lead to false detections of change.

We have studied changes in structure at the Coso geothermal area, in southeastern California, using microearthquake seismic tomography, but instead of inverting data sets from different epochs independently, we invert them simultaneously, seeking only those changes in structure that are required by the data. The algorithm, *tomo4d*, seeks to minimize the differences between derived models as well as to optimize the fit between observed and predicted arrival times. Tests using synthetic data show that the method is sensitive to small changes in wave speed but suppresses false alarms, i.e., changes in structure that are not required by the data. Recent additions to *tomo4d* include the ability to use data from regional as well as local earthquakes and to impose optional constraints on various measures of model complexity.

Coso is the seventh largest exploited geothermal area in the world. It is 28 km² (11 sq. miles) in area, and has a water-dominated reservoir with temperatures up to 349°C (660°F). The Coso field has produced electricity for more than two decades, and currently has 100 production wells up to 3.8 km (12,500 ft) deep that provide hot water and steam to generate 170 GMW (gross power generation) of electric power. In this paper we report in detail on studies of V_p , V_s , and V_p/V_s covering the epochs 1996, 2006, 2007, 2008, 2010, and 2012.

1. INTRODUCTION

It is expected that prolonged removal of geothermal fluids will change the states of geothermal reservoirs in ways that might be detectable using seismology. This occurs because the mechanical properties of porous rocks, which affect seismic wave-speeds, depend among other things on the nature of the pore fluids, which can change when geothermal exploitation depletes reservoirs faster than they are recharged by natural processes. Serendipitously, many exploited geothermal areas are seismically active, producing abundant microearthquake activity. This seismicity offers the tantalizing possibility of methods to monitor continuously changes within reservoirs as exploitation proceeds.

Developing seismological methods for measuring such changes has, however, not been straightforward. In one of the first studies, of The Geysers geothermal area, California, Gunasekera *et al.* (2003) used the method of repeat tomography using the well-established program *simulps12* (Thurber, 1983; Evans *et al.*, 1994). They inverted microearthquake *P*- and *S*-phase arrival times for different time periods (epochs) independently, and compared the final results, assuming that differences between the derived models reflect structural change in the reservoir.

Gunasekera *et al.* (2003) successfully applied this method to The Geysers using data from 1991 to 1998. They detected a clear, strong low- V_p/V_s anomaly in the shallowest 2 km (6500 ft) of the geothermal field that clearly expanded with time. The anomaly corresponded closely to the exploited reservoir, and expanded progressively with time. This result fit readily with seismic changes predicted for the depletion of liquid pore-fluid and its replacement with steam, a process known to be progressive and extreme at The Geysers.

Although successful when applied to The Geysers, this simple approach works only under ideal circumstances where the signal is strong and the experimental conditions unusually good, because tomographically derived structures can differ for reasons besides physical changes in the reservoir. These reasons include differences in seismic ray distributions from epoch to epoch resulting from differences in the locations of microearthquakes and of seismic stations, and to inevitable observational errors. These effects can cause large changes in the seismic structure derived that outweigh real changes in reservoir structure. Put another way, the effect of uncorrected errors can be much greater than that of the change in structure being sought.

These difficulties did not come to the fore in the study of Gunasekera *et al.* (2003) because structural change resulting from reservoir depletion during the 1990's were extremely strong while error sources were relatively modest. The reservoir was undergoing heavy progressive depletion and little replenishment via reinjection. Furthermore, the distribution of seismicity was

relatively stable and the seismic network dense, so that the data were highly redundant and ideal datasets could be selected for inversion.

Following that successful demonstration, the method of repeat tomography was applied to other promising targets, including the Coso geothermal area, California. This experiment immediately highlighted the fundamental difficulty explained above. Production at the Coso geothermal area is well-managed and the rate of reservoir depletion is much smaller than at The Geysers during the 1990's. Repeat tomography applied to the Coso geothermal area revealed changes in structure from year to year, but they were too modest to be confidently interpreted as real change in reservoir structure and not experimental error.

This experience inspired a long-term effort to develop rigorous methods for imaging reservoir change in exploited geothermal areas. Over the last several years, a programming tool was developed, tested with synthetic data and then applied to real data, a process that revealed the necessity for modifications and refinements that have occupied the last year or so. The mature program has recently been applied to the real datasets that comprise the first program application to such data, *i.e.*, data from Long Valley caldera, Mt. Etna, and the Coso geothermal area. This paper reports on the results from the latter target.

2. METHOD

The approach used by the new software has been described in detail in earlier publications (Julian and Foulger, 2010; Mhana *et al.*, 2017) and is briefly reiterated here. The computer program *tomo4d* overcomes the problems of inhomogeneous ray distributions between epochs by inverting data sets from pairs of epochs simultaneously, imposing constraints to minimize differences between the models derived. This approach amounts to interrogating the data to test whether changes in structure are *required* by the data, in contrast to testing whether structural changes are *permitted* by the data.

Real seismic datasets contain only a small amount of information compared with what would be required to fully specify a detailed three-dimensional model of Earth structure. In practice, there are always an infinite number of significantly different three-dimensional models that fit a set of observations within its uncertainties. Selecting only one of these many different tomographic models permitted by the data for interpretation is thus not a safe way forward. The approach used by *tomo4d*, of finding the smallest temporal changes consistent with the observations, is a safe, conservative approach that attempts to test specific hypotheses by falsifying possible models, as advocated by Tarantola (2006).

Performing the necessary computations requires solution of systems of linear algebraic equations whose order is twice that required for a single epoch of data. Fortunately, the additional sub-matrices involved are sparse, making possible optimizations that largely eliminate this problem. *tomo4d* incorporates additional improvements over other commonly used local-earthquake tomography programs, *e.g.*, by using exact ray tracing through 3D structures instead of approximations (Julian and Gubbins, 1977). In its current form, *tomo4d* takes approximately 30 minutes to process two epochs of Coso data on a modern laptop computer.

3. THE COSO GEOTHERMAL AREA AND EARLY TOMOGRAPHIC WORK

The Coso geothermal area is located near the southwestern corner of the Basin and Range province in southeastern California (Figure 1). It is commercially exploited and an area of intense microearthquake activity. The geothermal field lies on the Naval Weapons Center, and the seismometer network operated by the Geothermal Program Office of the US Navy records thousands of earthquakes per year.

Foulger (2007) studied the area using the same method that had been successfully applied to The Geysers by Gunasekera *et al.* (2003). They performed independent tomographic inversions of high-quality subsets of *P*- and *S*-phase arrival-time data from each of the nine years 1996-2004. The results provided evidence for an irregular reduction of the wave-speed ratio V_P/V_S in the upper 2 km (6500 ft) of the geothermal field. However, the lack of consistency from year to year undermined confidence in the results and motivated development of a more rigorous method—the *tomo4d* algorithm.

2. ANALYSIS OF DATA FROM THE COSO GEOTHERMAL AREA

2.1 Earthquake Data and Damping Parameters

We studied the years 1996, 2006, 2007, 2008, 2010, and 2012. All the data were collected on the three-component borehole seismometer network of the U. S. Navy Geothermal Program Office. Datasets comprising several hundred of the best-recorded earthquakes for each year, well distributed throughout the study volume, were selected for inversion. In order to obtain the best distribution we divided the study volume into 200 boxes (Figure 2), and selected the 10 best events in each, ranking events by the number of arrival-time measurements, smallness of the root-mean-square arrival-time residuals, smallness of the largest azimuthal gap between seismometers, and event magnitude.

Only hand-measured *P*- and *S*-phase arrival times were used. Those for 1996, 2006 and 2007 were measured by personnel of the U. S. Navy Geothermal Program Office. The other epochs were measured by the first author of this paper, using the interactive seismogram-analysis program *epick*. The precision to which arrival times could be measured is ~ 0.01 s for *P* phases and ~ 0.3 s for *S* phases.

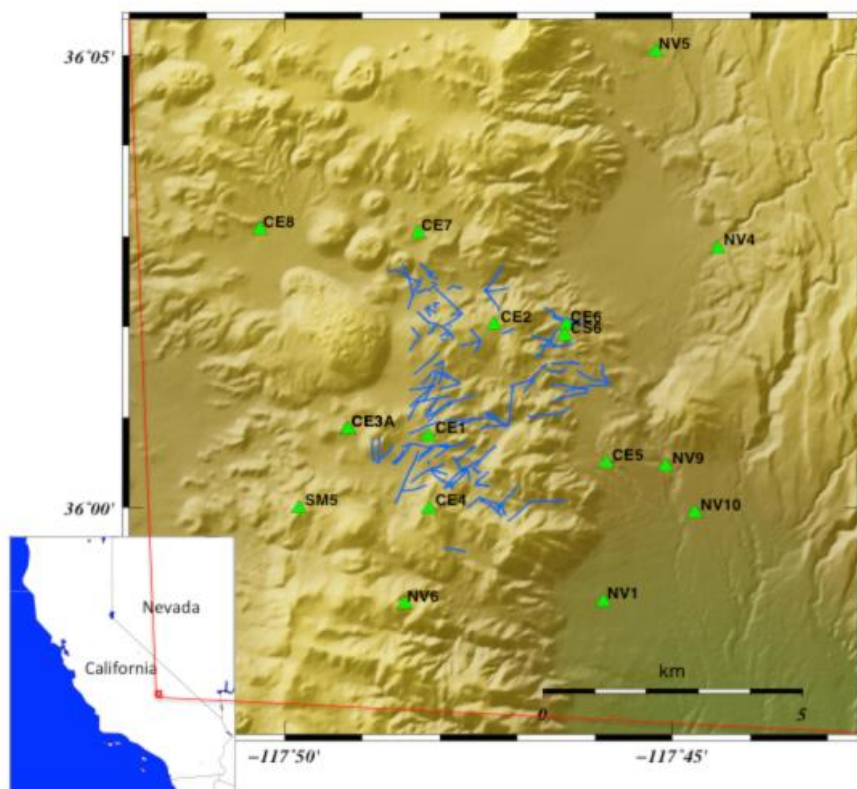


Figure 1: Shaded relief map of the Coso geothermal area. Green triangles: seismometer stations; blue lines: surface projections of geothermal wells. Inset shows the regional location of the main map.

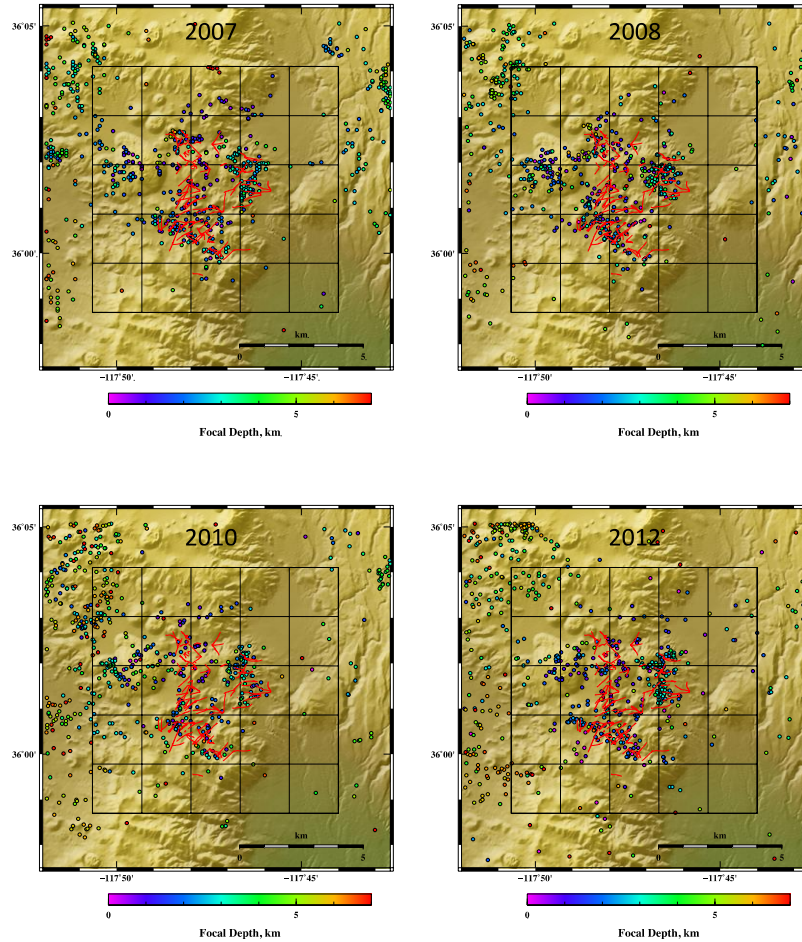


Figure 2: Earthquakes analyzed for the years 2007, 2008, 2010 and 2012, color-coded by focal depth, and the 10 km × 10 km × 8 km (32,808 ft × 32,808 ft × 26,246 ft) tomographic grid that parameterizes the study volume. Red lines: surface projections of geothermal boreholes.

tomo4d controls the magnitudes of perturbations made to event origins, seismic wave-speeds, and inter-epoch wave-speed differences using a multi-component objective function. Values must thus be chosen for three damping parameters. We made these selections by first performing single-iteration inversions using a range of values and examining the trade-offs between goodness of fit and origin and model perturbations. The results of such tests for the data from 1996 and 2006 are shown in Figure 3.

2.2 Hit Counts and Quality of the Results

The numbers of ray paths passing near each node of the tomographic grid are plotted as ray-density maps in Figure 4. This figure illustrates the sampling achieved for the target volume. The best-sampled area for 2007 and 2012 is the main geothermal field down to 1 km (3300 ft) below sea level. (The surface in the area lies about 1 to 1.5 km (3300 to 4900 ft) above sea level.). This is the region best illuminated by seismic rays because most of the microearthquakes are (probably) induced in the geothermal area in the volume from which fluids are mined. The density of sampling begins to deteriorate at 2 km (6500 ft) below sea level and is poor at depths greater than this. Ray coverage for *S* phases is of similar quality to that of *P* phases as a result of the high quality of the three-component borehole seismometers that comprise the network at Coso.

Satisfactory reduction in data residuals was achieved. Such reductions are related to the quality of the initial arrival-time data used, so a large reduction does not necessarily mean a good result but can indicate noisy initial input data. The final RMS travel-time residual is a better indication of the goodness of fit to the data of the final model. For the 2007 data the final RMS residual was ~0.04 s for *P* arrival times and ~0.07 s for *S* arrival times. For 2012 these values were ~0.03 s and ~0.04 s. The higher final RMS for *S* residuals is a consequence of those arrival times having larger measurement errors because the *S* wave arrives in the wave train of the earlier *P* arrival.

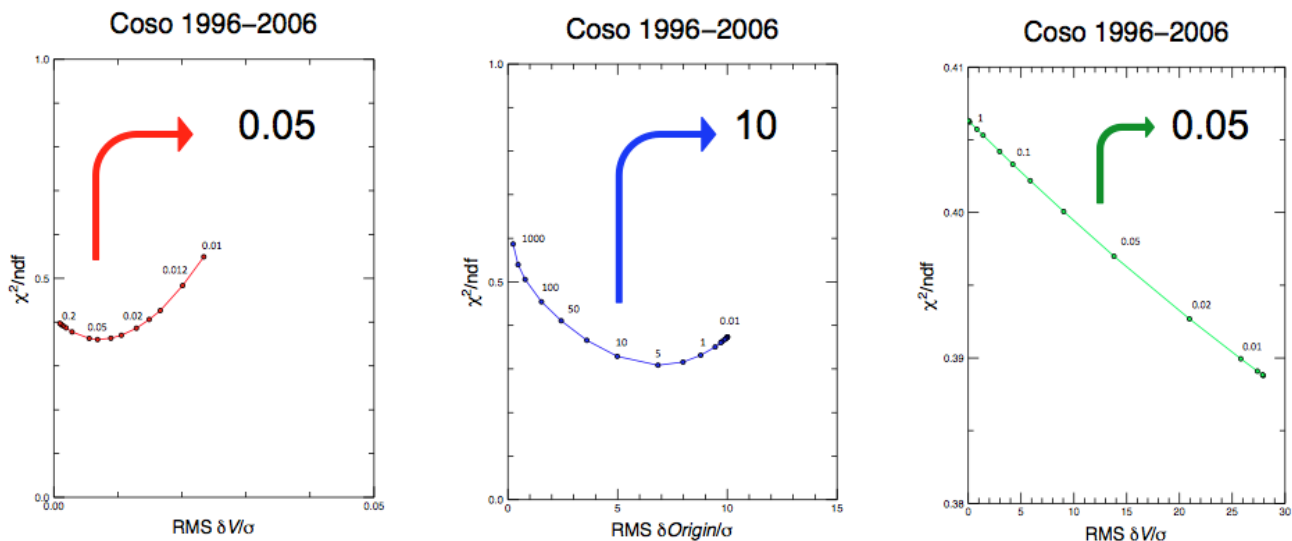


Figure 3: Trade-off damping curves for wave speeds (left), event origins (middle), and inter-epoch wave-speed changes (right) for data from the years 1996 and 2006. The optimal damping values chosen are indicated.

3. RESULTS

3.1 Structural Changes Between 2006 and 2012

We discuss only the well-sampled region in the center of our tomography grid, which corresponds approximately to the producing geothermal field. Our tomographic method is designed to seek preferentially solutions with small changes in structure. The method was, however, unable to do totally eliminate such changes. Clear, systematic changes in seismic wave speeds were required for the series of epochs 2006 - 2007 - 2008 - 2010 - 2012 (Figure 5).

The best-sampled central part of the imaged region can be divided into two parts on the basis of the style of structural change detected for this 6-year period: the northeast part and the southwest part. The northeast part is characterized by a relatively stable V_P and a systematic reduction in V_S , resulting in a net progressive increase in V_P/V_S . The southwest part behaved in the opposite fashion. V_P decreased progressively while V_S changed little during the same period, resulting in a progressive reduction in V_P/V_S . These changes occurred consistently, with progressively increasing strength, throughout the six-year period.

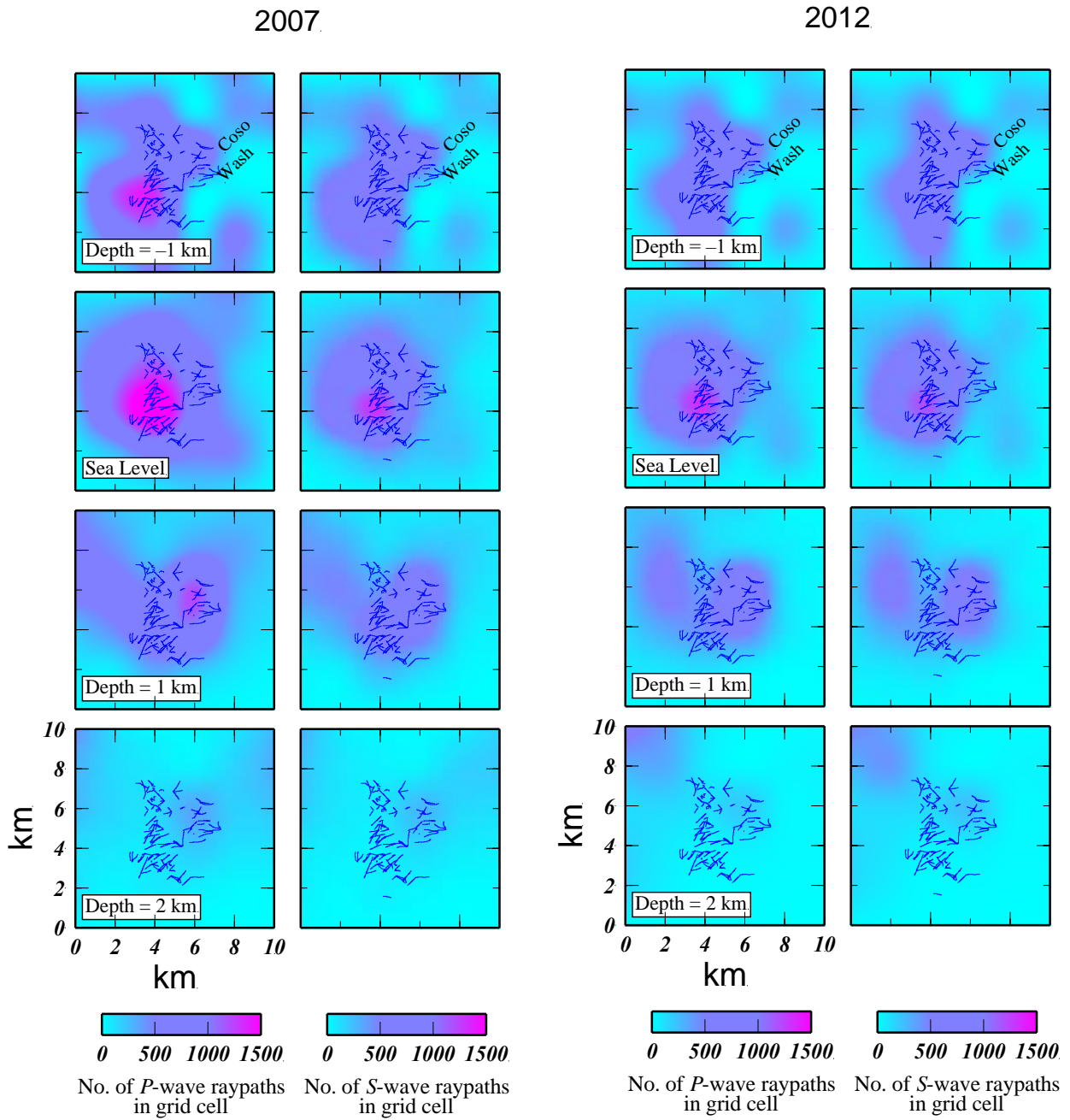
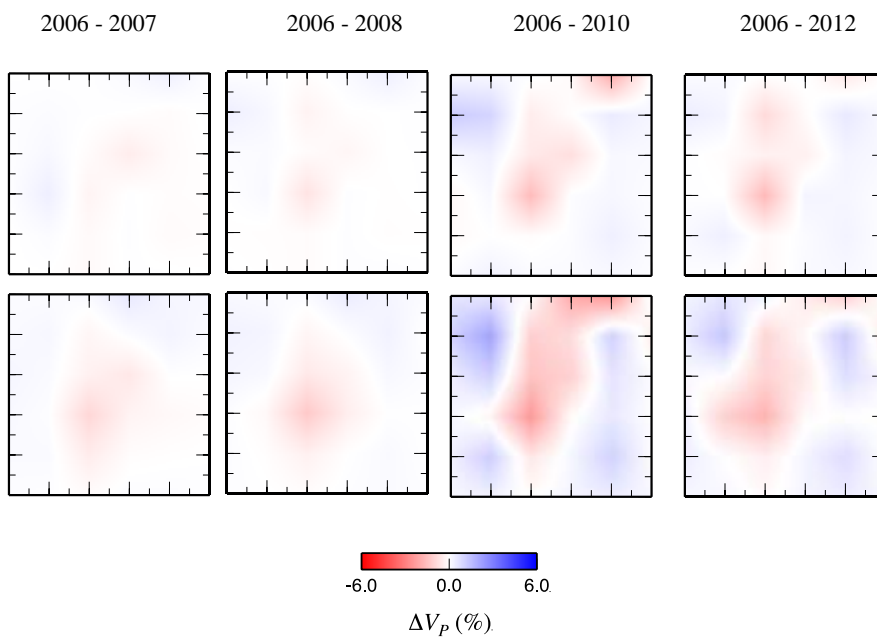
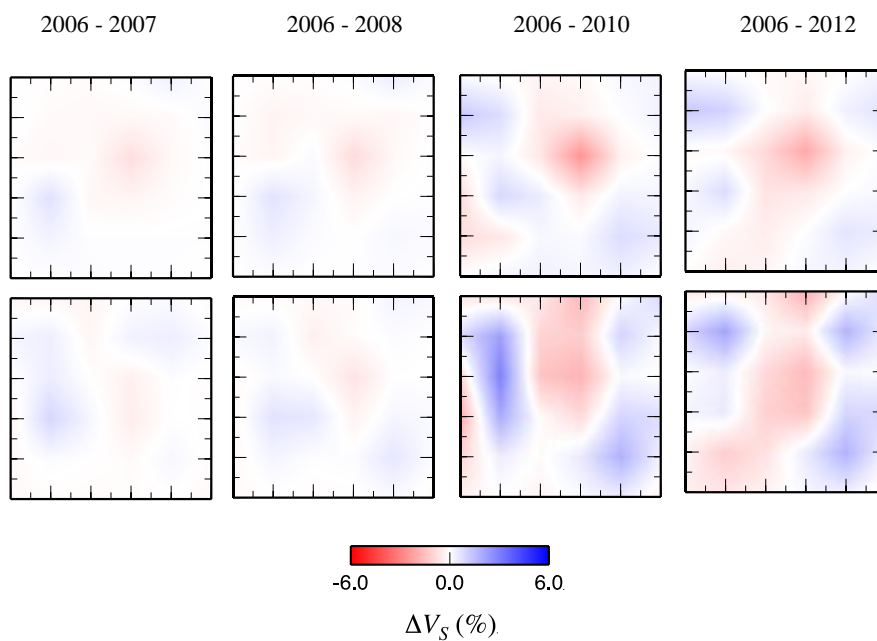


Figure 4: Hit-count maps indicate the best-sampled parts of the study volume at various depths for the epochs 2007 (left pair of columns, left *P*, right *S*) and 2012 (right).

(a) Changes in V_p



(b) Changes in V_s



(see following page for caption)

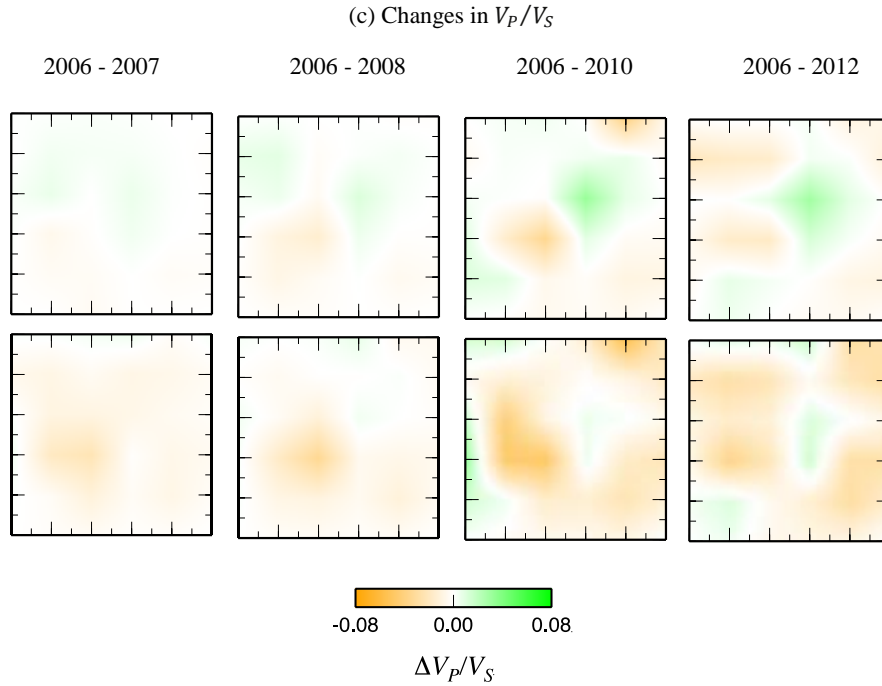


Figure 5. Top: (a) Changes in V_p for the epochs 2006-2007, 2006-2008, 2006-2010 and 2006-2012 for (top row) the 1-km (3280 ft) thick layer from 1 to 0 km (0 - 3280 ft) above sea level and (bottom row) the 1-km-thick (3280 ft) layer from 0 km to 1 km (0 - 3280 ft) below sea level. (b) same as (a) for V_s . (c) Same as (a) for V_p/V_s .

Table 1 shows a suite of processes likely to occur in producing geothermal fields. The results described above may be interpreted in this framework as follows. For the northeast part of the reservoir, the relatively small change in V_p , the large reduction in V_s and consequential increase in V_p/V_s is consistent with pressure increase and fracturing. For the southwest part of the reservoir, the relatively large decrease in V_p , coupled with a small lowering of V_s and consequential decrease in V_p/V_s is consistent with steam replacing water in this part of the field.

Table 1. The effects upon V_p , V_s and V_p/V_s of processes that occur in geothermal areas. Large arrows indicate the dominant effects, and small arrows indicate weaker or negligible effects. Blue oval: structural changes observed to occur in the top 2 km (6560 ft) of the northeast part of the producing field. Red oval: changes observed in the southwest part of the field.

	V_p	V_s	V_p/V_s
Water saturation	↑	—	↑
Pressure increase and fracturing	↓	↓	↑
Pore pressure decrease	↑	↑	↓
Drying of minerals	↑	↑	↓
Temperature decrease	↑	↑	↓
Steam replacing water	↓	↓	↓

3.2 Structural Changes Between 1996 and later epochs

We also processed seismic data from Coso gathered in 1996 and calculated changes for the later years 2006, 2007, 2008, 2010 and 2012. The results obtained are different from, and inconsistent with, the clear and systematic variations found for epochs from 2006 and later. The 1996 data differ from the later years. They were collected relatively early in the history of the seismic network at Coso. Furthermore they were not hand-measured by the first author of this paper, but imported from an existing catalog. These

factors may indicate that the data from 1996 are of insufficient quality for the tomographic method. Further examination of the 1996 data is necessary in order to understand better their suitability for this type of work.

4. FUTURE WORK

A vast database of microearthquake data is available for the Coso geothermal field, for every year from 1996 through 2017. Given the significance of the present result it would be of extreme interest to process additional data from the years not studied yet, to better assess the time-series of structural change.

In collaboration with the producers, correlations between production, reinjection and structural change should be sought. This work would potentially allow changes in seismic structure to be interpreted numerically in terms of lost pore fluid. In this way, the new method may be developed into a tool that can quantify the progression of reservoir depletion hand-in-hand with production.

3. CONCLUSIONS

We have successfully imaged in three dimensions systematic and progressive changes in seismic wave-speeds at the Coso geothermal field during ongoing production. The strength of the structural-change anomaly is small and not possible to detect using the traditional method of differencing independently derived three-dimensional models. We developed a new tool, *tomo4d*, which is much more sensitive and able to distinguish subtle changes in structure from the much larger errors inherent in the traditional method.

To our knowledge, this is the first reliable report of such subtle changes in Earth structure. Additional inversions for earlier years, using data of similar quality to those from 1996 and later, is an exciting potential research task for the future. *tomo4d* should also be applied to other geothermal areas where production is thought to produce structural changes, *e.g.*, The Geysers.

REFERENCES

- Evans, J. R., D. Eberhart-Phillips, and C. H. Thurber (1994), User's manual for SIMULPS12 for imaging V_P and V_P/V_S , a derivative of the Thurber tomographic inversion SIMUL3 for local earthquakes and explosions, Open-file *Report 94-431*, 142 pp., US Geological Survey.
- Gunasekera, R. C., G. R. Foulger, and B. R. Julian (2003), Reservoir depletion at The Geysers geothermal area, California, shown by four-dimensional seismic tomography, *J. Geophys. Res.*, **108**(B3), 2134, doi:2110.1029/2001JB000638.
- Foulger, G. R., B. R. Julian, A. M. Pitt, D. P. Hill, P. E. Malin, and E. Shalev (2003), Three-dimensional crustal structure of Long Valley caldera, California, and evidence for the migration of CO₂ under Mammoth Mountain, *J. Geophys. Res.*, **108**(B3), 2147, doi:2110.1029/2000JB000041.
- Foulger, G. R. (2007), Report to the U.S. Geological Survey on time-dependent seismic tomography of the Coso geothermal area, Inyo County, CA covering the years 1996-2006, Technical Rep., iv+119 pp, U.S. Geological Survey, Menlo Park, California.
- Julian, B. R., and D. Gubbins (1977), Three-dimensional seismic ray tracing, *J. Geophys.*, **43**(1/2), 95-113.
- Julian, B. R., G. R. Foulger, K. Richards-Dinger, and F. Monastero, Time-dependent seismic tomography of the Coso geothermal area, 1996-2004, *Proceedings*, 31st Workshop on Geothermal Reservoir Engineering, Stanford University, Stanford, CA (2006).
- Julian, B. R., and G. R. Foulger (2010), Time-dependent seismic tomography, *Geophys. J. Int.*, **182**(3), 1327-1338.
- Mhana, N., B.R. Julian, G.R. Foulger and A. Sabin, Monitoring Geothermal Reservoir Depletion Using Time-dependent Seismic Tomography, *Proceedings*, 42nd Workshop on Geothermal Reservoir Engineering, Stanford University, Stanford, CA (2017).
- Tarantola, A. (2006), Popper, Bayes and the inverse problem, *Nature Physics*, **2**, 492-494.
- Thurber, C. H. (1983), Earthquake locations and three-dimensional crustal structure in the Coyote Lake area, central California, *J. Geophys. Res.*, **88**, 8226-8236.